

# Federated Ensemble Model-based Reinforcement Learning

Jin Wang, Jia Hu, Jed Mills, and Geyong Min

**Abstract**—Federated learning (FL) is a privacy-preserving machine learning paradigm that enables collaborative training among geographically distributed and heterogeneous users without gathering their data. Extending FL beyond the conventional supervised learning paradigm, federated Reinforcement Learning (RL) was proposed to handle sequential decision-making problems for various privacy-sensitive applications such as autonomous driving. However, the existing federated RL algorithms directly combine model-free RL with FL, and thus generally have high sample complexity and lack theoretical guarantees. To address the above challenges, we propose a new federated RL algorithm that incorporates model-based RL and ensemble knowledge distillation into FL. Specifically, we utilise FL and knowledge distillation to create an ensemble of dynamics models from clients, and then train the policy by solely using the ensemble model without interacting with the real environment. Furthermore, we theoretically prove that the monotonic improvement of the proposed algorithm is guaranteed. Extensive experimental results demonstrate that our algorithm obtains significantly higher sample efficiency compared to federated model-free RL algorithms in the challenging continuous control benchmark environments. The results also show the impact of non-IID client data and local update steps on the performance of federated RL, validating the insights obtained from our theoretical analysis.

## I. INTRODUCTION

Federated Learning (FL) has emerged as an important Machine Learning (ML) paradigm that aims to collaboratively train ML models in a distributed fashion without sensitive data leaving the user devices. Many popular FL algorithms, such as Federated Averaging (FedAvg) [1], work iteratively with rounds of local training on clients followed by model uploading and aggregation on a server. Thus, only model parameters instead of sensitive user data are uploaded by clients to the server. The majority of FL works [2], [3], [4] consider training supervised learning models for solving perception problems such as image classification and linguistic prediction.

More recently, federated Reinforcement Learning (RL) was proposed to extend FL to train RL models to solve sequential decision-making problems. The existing federated RL works [5], [6], [7] directly combine model-free RL with FL. Specifically, they train policies locally for all collaborating devices, using the model-free RL objective, and average the policy parameters on the server to generate a global policy for the next round of local training. However, traditional model-free RL generally has high sample complexity whilst obtaining samples is costly in many real-world scenarios (e.g., cloud

robotics [8] and autonomous driving [9]). Furthermore, the theoretical properties (such as monotonic improvement) of these federated model-free RL algorithms were not well understood. These issues hinder the use of federated model-free RL in real-world scenarios.

Compared to model-free RL, model-based RL methods [10], [11], [12] are much more sample efficient. Model-based RL learns an estimated dynamics model and then derives an optimal policy based on this model. Since the dynamics model is trained by using supervised learning, it can be naturally adapted to the current federated supervised learning setting where many state-of-the-art FL algorithms are available. Nonetheless, there are several major challenges for integrating model-based RL into FL.

First, model bias (caused by overfitting in regions where insufficient data is available to train the model) is a key factor that affects model-based RL methods [11]. Handling RL model bias in the federated setting is even more challenging due to the highly heterogeneous client datasets. Second, a rigorous theoretical analysis of federated RL is lacking. Especially, monotonic improvement of the algorithm has not been proved to hold in the federated setting. Third, it is unclear how non-Independent and Identically Distributed (non-IID) client data will affect the performance of federated model-based RL.

In this paper, we extend model-based RL to the FL paradigm, proposing a new Federated Ensemble Model-based Reinforcement Learning (FEMRL) algorithm. In FEMRL, the dynamics model is trained by FL, and then the RL policy is trained by solely using the dynamics model without interacting with the real environment. To address the problem of model bias, we create an ensemble of dynamics models uploaded by clients. In addition, an ensemble distillation method is used to improve the performance of model aggregation during FL. We summarise the key contributions of our work as follows:

- We propose a novel federated reinforcement learning algorithm, FEMRL. To the best of our knowledge, this is the first of its kind that effectively extends model-based RL to the popular FL setting. In particular, we leverage FL and knowledge distillation techniques to create an ensemble of dynamics models from clients, and then train the policy by solely using the ensemble without relying on sampling data from the real environment.
- We provide a rigorous theoretical analysis to prove that the monotonic improvement of FEMRL is guaranteed. The discrepancy bound of the return from the real environment and the learned dynamics identifies and highlights the impacts of non-IID client data on policy improvement for federated RL.

- We perform extensive experiments using four challenging continuous control environments [13], which demonstrate the superior sampling efficiency (hence lower computation and communication cost) of FEMRL compared to federated model-free RL algorithms. We also perform experiments to investigate the impacts of non-IID client data and local update steps on the rate of reward improvement for federated RL.

## II. RELATED WORK

**Federated Reinforcement Learning:** Several previous works have investigated training RL policies in the FL setting. [7] proposed a system for training virtual Pong players (controlled via a Deep Q-network) in the FL setting to match the skill levels of (simulated) players. [5] and [14] proposed federated RL algorithms for training policies to maximise content cache-hits on Base Stations at the network edge. [6] designed the FedRL system for training a policy, where individual FL clients do not have access to the full state-space of the RL task. While these works contribute to the development of model-free RL in the FL setting, they suffer from high sample complexity and lack theoretical guarantees.

**Model-based Reinforcement Learning:** RL algorithms are generally built on Markov Decision Processes (MDP) and can be divided into two categories: model-free RL algorithms, which directly train a value function or policy by trial-and-error in the environment; and model-based RL algorithms that explicitly learn a dynamics model based on the sampled data and derive a policy from the model. Model-based RL has been demonstrated to have significantly higher sample efficiency than model-free RL, and has been successfully applied to robotics [15], video games [12], etc., using a variety of dynamics models including Gaussian processes [16], linear models [17], [18], mixtures of Gaussians [19], and Deep Neural Networks (DNNs) [20], [21], [22]. One key challenge for model-based RL is how to handle uncertainty of the dynamics model [11], [23]. To address this challenge, ensembles of DNNs [11], [23], [15] have been used to handle model uncertainty given data collected from the environment. In our FEMRL algorithm, we approximate the model dynamics using DNNs and create an ensemble using the models uploaded by FL clients. From the theoretical perspective, previous works [24], [10], [25], [26] have provided general frameworks for analysing model-based RL, which include monotonic improvement guarantees. We extend the analyses of these works to our FEMRL algorithm, proving the monotonic improvement of FEMRL, which also demonstrates the influence of non-IID client data on the policy improvement.

**Federated Ensemble Distillation:** FL aims to train a global model by sharing users' locally-trained models, rather than their private data. A crucial step in FL is how to aggregate local models into a global model. The seminal FedAvg algorithm [1] averages local models after each communication round to produce a new global model. However, directly averaging model parameters may not be the most effective method of creating the

global model, due to non-IID client data, which is a significant challenge in FL and can come in many forms [27]. Some recent works focus on using ensemble distillation techniques to create more robust global models. [28] proposed a novel aggregation approach using Bayesian model ensembles and knowledge distillation. [29] proposed a similar algorithm for distillation on the server, using the average logits of the client models on an unlabelled dataset as the distillation target. Inspired by the above methods, we aggregate the client models into a single global model using knowledge distillation. Moreover, in our method, we sample fictional experience (as opposed to real experience) from the ensemble of models for knowledge distillation, further helps reduce the privacy risks of FEMRL.

## III. PRELIMINARIES

**Federated Learning:** In FL, clients collaboratively train a model without exchanging their training data in any way. The FL objective is to find the minimiser  $\mathbf{w}$  of the average client loss function  $f$ :

$$\min_{\mathbf{w} \in \mathbb{R}^d} f(\mathbf{w}) = \frac{1}{K} \sum_{k=1}^K p_k f_k(\mathbf{w}), \quad (1)$$

where  $K$  is the total number of clients,  $p_k$  and  $f_k$  are the fraction of total samples ( $\sum_k p_k = 1$ ) and average loss over samples on client  $k$ , respectively. Therefore, FL aims to compute the minimiser of the average loss over all samples on all participating clients (i.e., the same objective as would be achieved by centralised training on pooled data). However, in real-world FL data is non-IID across clients, as the behaviour of each client influences how its local samples are generated. Non-IID client data has been extensively shown to hinder the convergence of the FL model, and is one of the key challenges to FL. In our FEMRL algorithm, we use FL to train the dynamics model of the MDP.

**Reinforcement Learning:** A sequential decision-making problem solved by RL is generally modelled as an MDP, which is given by the six-tuple  $\mathcal{M} := (\mathcal{S}, \mathcal{A}, T, R, \rho_0, \gamma)$ . Here,  $\mathcal{S}$  and  $\mathcal{A}$  are the state and action spaces, respectively.  $T(s'|s, a)$  represents the dynamics that specifies the conditional distribution of the next state  $s'$  given the current state  $s$  and action  $a$ .  $R(s, a)$  is the reward function,  $\rho_0$  represents the initial state distribution, and  $\gamma \in (0, 1)$  denotes the discount-factor. Denote  $\pi(\cdot|s)$  as the policy that specifies the conditional distribution over action space given a state  $s$ . The goal of RL algorithms is to find the optimal policy that maximises the expected discounted return defined by  $\mathbb{E}_{\pi, T, \rho_0} [\sum_{t=0}^{\infty} \gamma^t R(S_t, A_t)]$ . Define the value function following policy  $\pi$  with MDP  $\mathcal{M} := (\mathcal{S}, \mathcal{A}, T, R, \rho_0, \gamma)$  as:

$$V_{\pi}^{\mathcal{M}}(s) = \mathbb{E}_{\substack{S_{t+1} \sim T(\cdot|S_t, A_t) \\ A_t \sim \pi(\cdot|S_t)}} \left[ \sum_{t=0}^{\infty} \gamma^t R(S_t, A_t) \middle| S_0 = s \right]. \quad (2)$$

Thus  $V_{\pi}^{\mathcal{M}} := V_{\pi}^{\mathcal{M}}(s_0)$  is the total return given policy  $\pi$ , where  $s_0 \sim \rho_0$  is the initial state.

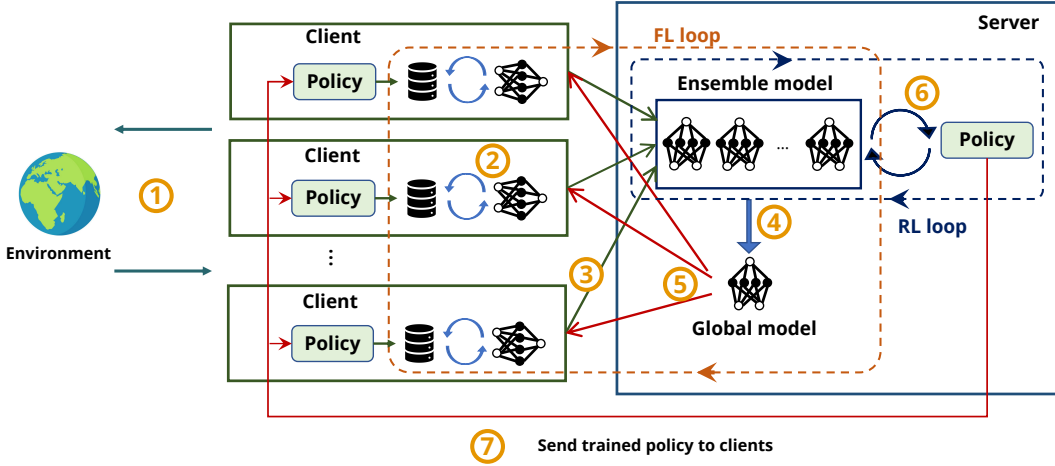


Figure 1: Overview of the FEMRL algorithm. **Step 1:** each client samples data from the real environment based on the local sample policy and stores the data locally. **Step 2:** local dynamics models are trained based on the sampled data. **Step 3:** the parameters of the local dynamics models are sent to the server. **Step 4:** an ensemble of dynamics models are created on the server using the uploaded client models, and a single global model is then created via knowledge distillation. **Step 5:** the parameters of the global model are sent to clients. Then, starting step 2 again for  $T_c$  rounds of FL loops. **Step 6:** after rounds of FL training, the server then trains the policy using a policy-gradient algorithm (e.g., TRPO) and the ensemble of dynamics models. **Step 7:** the parameters of the new policy are sent to clients for the next round of sampling (i.e., Step 1).

#### IV. FEDERATED ENSEMBLE MODEL-BASED REINFORCEMENT LEARNING (FEMRL)

In this section, we first propose the FEMRL algorithm, and then provide a theoretical analysis guaranteeing monotonic improvement of the policy produced by FEMRL.

##### A. Algorithm Design

Our algorithm intends to train a model-based RL policy in an edge-computing environment involving multiple client devices, and a corresponding edge server. In our setting, all participating clients share the same MDP dynamics. There are many real-world applications corresponding to this setting, including Unmanned Aerial Vehicles [30], edge caching [5], and resource management in edge-computing systems [31]. Fig. 1 illustrates the operation of FEMRL, which consists of two major sub-components: FL loop for the training of dynamics model, and RL loop for policy training.

Formally, define the MDP with learned dynamics  $\hat{T}(s'|s, a; \mathbf{w})$  as  $\mathcal{M} := (\mathcal{S}, \mathcal{A}, \hat{T}, R, \rho_0, \gamma)$ , where  $\mathbf{w}$  are the parameters of the learned model. Define  $\hat{T}(s, a; \mathbf{w})$  as the function that produces the unique value of  $s'$ . The goal of the FL loop is to learn the optimal  $\mathbf{w}$  such that the discrepancy between the learned dynamics and real dynamics is minimal. This minimisation is a typical supervised learning process, which can be solved through maximum likelihood estimation or other techniques from generative and dynamics modelling. In this paper, we apply a multi-step prediction loss that is similar to [24] for model learning, and use a predefined reward function, as in the works [11], [23], [24]. Concretely, for a state  $s_t$  and action sequence  $a_{t:t+h}$ , the  $h$ -step prediction  $\hat{s}_{t+h}$

as  $\hat{s}_t = s_t$ , and for  $h \geq 0$ ,  $\hat{s}_{t+h+1} = \hat{T}(\hat{s}_{t+h}, a_{t+h}; \mathbf{w})$ , the  $h$ -step loss is defined as:

$$f(\mathbf{w}) = \frac{1}{H} \sum_{i=1}^H \|(\hat{s}_{t+i} - \hat{s}_{t+i-1}) - (s_{t+i} - s_{t+i-1})\|_2. \quad (3)$$

The FL loop involves  $T_c$  rounds of communication between client devices and the server. Within each round, each client trains a local dynamics model via Stochastic Gradient Descent (SGD) following the loss function given by Eq. (3) and using the samples local to that client. After local training, clients upload the model parameters to the server. All uploaded models are then aggregated into a single global model on the server-side. Instead of simply averaging the local models as in FedAvg [1], we create an ensemble model  $\{\mathbf{w}_k\}_{k=1}^m$  based on the uploaded local models, where  $\mathbf{w}_k$  is the local model updated by the  $k^{\text{th}}$  client. This ensemble serves two purposes: 1) creating a single global dynamics model that benefits from knowledge distillation; 2) generating fictitious data for policy training. Using the model ensemble, therefore, benefits both the FL and policy training processes by producing a robust aggregate model and alleviating the model bias problem in policy training.

The ensemble knowledge distillation method involves a typical student-teacher learning scheme. Denote the sampled fictitious data as  $\tau = \{s_0, a_0, \dots, s_n, a_n\}$ ,  $s_0 \sim \rho_0$ ,  $a_t \sim \pi(a_t|s_t)$ ,  $s_{t+1} = \hat{T}(s_t, a_t; \{\mathbf{w}_k\}_{k=1}^m)$ . The student model (i.e., the single global dynamics model) is trained with Adam [32] following the loss function:

$$L(\bar{\mathbf{w}}_t) = \left\| \frac{1}{m} \sum_{k=0}^m T(s_t, a_t; \mathbf{w}_k) - T(s_t, a_t; \bar{\mathbf{w}}_t) \right\|_2, \quad (4)$$

where  $T(s_t, a_t; \mathbf{w}_k)$  is the learned local dynamics of client  $k$  and  $T(s_t, a_t; \bar{\mathbf{w}}_t)$  is the global dynamics represented by the student model.

**Algorithm 1** FEMRL running on  $K$  clients (indexed by  $k$ ) for  $E$  epochs, each consisting of  $T_c$  rounds of federated communication and  $G$  steps of policy update. The dynamics and policy are initialized as  $w_0$  and  $\theta_0$ .

**Procedure FEMRL**

```

for  $n_{\text{outer}}$  epochs do
  Clients sample environment data using their policies
  for  $n_{\text{inner}}$  iterations do
     $\{w^{(k)}\}_{k=1}^K \leftarrow \text{FedEnLearning}(T_c)$ 
    for  $j \leftarrow 1$  to  $G$  do
      Generate fictitious samples  $\mathcal{D}$  using  $\pi_\theta$  and
      model ensemble  $\{w^{(k)}\}_{k=1}^K$ 
      Update policy  $\pi_\theta$  using TRPO and  $\mathcal{D}$ 
    Send the updated policy  $\pi_\theta$  to clients with synchronous
    rate  $\alpha$ .

```

**Procedure FedEnLearning ( $T_c$ )**

```

for  $t \leftarrow 1$  to  $T_c$  do
  for each client  $k \in K$  in parallel do
     $\triangleright$  LocalUpdate is detailed in Algorithm 2
     $w_k \leftarrow \text{LocalUpdate}(k, \bar{w}_{t-1}, E)$ 
  Create ensemble of models  $\{w_k\}_{k=1}^K$ 
  Initialize student model  $\bar{w}_{t,0} \leftarrow \frac{1}{|K|} \sum_k w_k$ 
  for  $j \leftarrow 1$  to  $N$  do
    Generate fictitious trajectories  $\tau$  using  $\pi_\theta$  and model
    ensemble  $\{w_k\}_{k=1}^K$ .
    Update the student model  $\bar{w}_t$  using loss function
    from Eq. (4) on  $\tau$ .
   $\bar{w}_t \leftarrow \bar{w}_{t,N}$ 
return  $\{w_k\}_{k=1}^K$ 

```

After  $T_c$  rounds of the FL loop, we then use a policy-gradient algorithm to train the policy by interacting with the ensemble of models. In this paper, we use Trust Region Policy Optimization (TRPO) [33] as the training algorithm. Next, the parameters of the updated policy are sent to all clients. Note that we do not restrict the policy at clients update to be a synchronous process, and only a fraction  $\alpha$  of clients may receive and update their policy each training epoch. Our design is practical since clients can be unreliable edge devices and may not always be able to reach the server (e.g., a smartphone loses cellular connection) in the FL scenario. We present the detailed server-side algorithm of FEMRL in Algorithm 1 and client-side algorithm in Algorithm 2 (see Appendix D). Specifically, we conduct training with  $n_{\text{outer}}$  epochs. Each epoch involves  $n_{\text{inner}}$  rounds of inner loops. Within each inner loop, we alternatively conduct  $T_c$  rounds of FL loops and  $G$  rounds of RL loops. In the following sections, we provide a theoretical guarantee of monotonic policy improvement for FEMRL, before performing a thorough empirical evaluation of the algorithm.

**B. Theoretical analysis**

Proving monotonic improvement guarantee is an important aspect of RL algorithms. In this section, we provide the conditions under which FEMRL is guaranteed to provide monotonic improvement for  $\pi$ . To prove monotonic improvement of a

model-based RL algorithm, we wish to find a lower bound of  $V_\pi^{\mathcal{M}}$ :

$$V_\pi^{\mathcal{M}} \geq V_\pi^{\widehat{\mathcal{M}}} - B \quad (5)$$

where  $B$  is the bounded value.

Since the model is trained with supervised learning, the distance between the true model and the learned model can be quantified by standard Probably Approximately Correct (PAC) generalization error [34]. PAC bounds the difference in generalisation and empirical error by a constant with high probability. In FEMRL, this generalisation error can be defined as the distance between the learned dynamics and the real environment dynamics. The recent literature provides two main ways to measure this distance, each with different assumptions. One assumes that the dynamics model is a complex probability distribution, and measures the distance using Total Variation Distance (TVD) [10]. The other assumes deterministic dynamics and directly uses 1-Wasserstein distance [24]. In addition, [35] uses a general measurement, Integral Probability Metric, where TVD and 1-Wasserstein distance are two special cases. Since TVD requires weaker assumptions and is typically more practical than 1-Wasserstein distance, we use TVD in our analysis. Overall, we make the following assumptions:

**Assumption 1.** The generalisation error is measured by the TVD, defined as  $\epsilon_m := D_{\text{TVD}}(\widehat{T}(\cdot|s, a)|T(\cdot|s, a)) = \frac{1}{2} \sum_{s'} |\widehat{T}(s'|s, a) - T(s'|s, a)|$

**Assumption 2.** The dependency of two policies  $\pi$  and  $\pi_D$  is measured by the TVD  $\epsilon_\pi = D_{\text{TVD}}(\pi(a|s)|\pi_{r_m D}(a|s))$ , and is bounded by a constant  $\delta_\pi$ , where  $D_{\text{TVD}}(\pi(a|s)|\pi_D(a|s)) \leq \delta_\pi$ .

**Assumption 3.** The reward function of the MDP is bounded:  $\forall s \in \mathcal{S}, \forall a \in \mathcal{A}, R(s, a) \leq r_{\max}$ .

**Assumption 4.** The loss function of the FL dynamics model is convex and bounded by  $L$ ,  $|f(w)| \leq L, \forall w$ .

Based on previous works [10], [24], [35], we have the following Lemma to build the lower bound of the discrepancy of the total returns from the true model and the learned model in conventional model-based RL:

**Lemma IV.1.** Denote  $\epsilon_m$  as the generalization error of the dynamics model and  $\epsilon_m^{\max}$  as the maximal value of  $\epsilon_m$ . Denote  $\epsilon_\pi$  as the discrepancy between target policy  $\pi$  and sample policy  $\pi_D$ . For any policy  $\pi$ , the return of the real environment  $V_\pi^{\mathcal{M}}$  and the return of the learned dynamics  $V_\pi^{\widehat{\mathcal{M}}}$  are bounded as:

$$V_\pi^{\mathcal{M}} \geq V_\pi^{\widehat{\mathcal{M}}} - \underbrace{\left[ \frac{2\gamma r_{\max}}{1-\gamma} \epsilon_m + \frac{4\gamma^2 r_{\max}}{(1-\gamma)^3} \epsilon_\pi \epsilon_m^{\max} \right]}_B. \quad (6)$$

*Proof.* See Appendix B.  $\square$

Lemma IV.1 gives a theoretical guarantee for the monotonic improvement of the model-based RL algorithm. As long as we improve the returns under the learned model by more than  $B$ ,

we can guarantee improvement under the real environment [10]. The bound  $B$  is proportional to the generalization error of the dynamics model,  $\epsilon_m$ , and the discrepancy between the sample policy and target policy,  $\epsilon_\pi$ . However, Lemma IV.1 holds only if the generalization error  $\epsilon_m$  is bounded. Conventional model-based RL methods use normal centralised supervised learning to train the dynamics model, however, in FEMRL we use FL to train the dynamics model through an ensemble of models created from the clients' local models to approximate the learned model,  $\hat{T}(s'|s, a; \{\mathbf{w}^{(k)}\}_{k=1}^K)$ . Therefore, it is necessary to investigate if  $\epsilon_m$  is bounded in the FL setting and what factors influence  $\epsilon_m$  in FEMRL.

We now derive a bound on the generalisation error of the ensemble of client models.

**Theorem IV.2.** *Denote the global data distribution as  $D$ . Let  $D_k$  be the local data distribution of client  $k$ . Let  $\pi_D^k$  be the sample policy for client  $k$ . Let  $\bar{\pi}_D$  be the virtual global sample policy. Therefore, we have  $D = \mathbb{P}_{s,a,s'} = \sum_{s,a} T(s'|s, a)\bar{\pi}_D(a|s)$  and  $D_k = \mathbb{P}_{s,a,s'} = \sum_{s,a} T(s'|s, a)\pi_D^k(a|s)$ . Denote  $S_k \sim D_k^m$  as local empirical distribution for client  $k$ . Let  $\hat{S}$  be the global empirical distribution, each local empirical distribution has equal contribution to the global distribution, thus  $\hat{S} = \frac{1}{K} \sum_{k=1}^K S_k$ . Let  $\mathcal{H}$  be a hypothesis class with limited Vapnik–Chervonenkis (VC) dimension,  $VCdim(\mathcal{H}) \leq d < \infty$ . The hypothesis  $h \in \mathcal{H}$  learned on  $S_k$  and  $\hat{S}_k$  is denoted by  $h_{S_k}$  and  $\hat{h}_{S_k}$ , respectively. Then, the generalisation error of the ensemble model is bounded with probability at least  $1 - \delta$ :*

$$\begin{aligned} \epsilon_m &:= \epsilon_D \left( \frac{1}{K} \sum_k h_{S_k} \right) \\ &\leq \epsilon_{\hat{S}_k}(h_{\hat{S}_k}) + C \sqrt{\frac{d + \log(1/\delta)}{m}} + \frac{L}{K} \Gamma, \end{aligned} \quad (7)$$

where  $C$  and  $L$  are constants,  $m$  is the number of training samples per local data distribution, and  $\Gamma = \sum_{k=1}^K D_{\text{TV}}(\bar{\pi}_D || \pi_D^k)$ .

*Proof.* See Appendix B.  $\square$

Theorem IV.2 shows the generalisation error is bounded, thus the monotonic improvement (i.e., Lemma IV.1) still holds for FEMRL. There are three key factors affecting the maximal value of generalisation error  $\epsilon_m$ : the virtual global empirical error  $\epsilon_{\hat{S}_k}(h_{\hat{S}_k})$ , the number of training samples  $m$ , and the sum of TVDs between the clients' sample policies and the virtual global sample policy,  $\Gamma$ .

Note that, The virtual global empirical error can in principle be estimated and optimised approximately by the training loss.  $\Gamma = \sum_k D_{\text{TV}}(\bar{\pi}_D || \pi_D^k) = \sum_k \|D - D_k\|_1$  can be a measurement of the degree of non-IID of clients' datasets. When the data distribution is IID on all clients,  $\|D - D_k\|_1 = 0$ ,  $D_{\text{TV}}(\bar{\pi}_D || \pi_D^k) = 0, \forall k$ , which means all clients share the same sample policy. When the data distribution of clients becomes heterogeneous,  $\Gamma > 0$ . Specifically, the higher degree of non-IID of data distribution, the higher  $\Gamma$  is.

In our algorithm, the degree of non-IID is mainly determined by policy synchronisation rate  $\alpha$ . Each epoch, assume  $\alpha$  fraction of clients update their policy using the newest global policy (the rest of the clients do not for various reasons, e.g., lost

of connection to server). For  $\alpha < 1$ , clients' data become non-IID, as some clients will be performing local updates on the environment model using a 'stale' (unsynchronised) policy. We now analyse the effect of policy synchronisation rate  $\alpha$  on the measure of non-IID client data distributions,  $\Gamma$ . Denote the sample policy before and after the global update as  $\pi_D$  and  $\pi'_D$ , respectively. After policy synchronisation (with rate  $\alpha$ ),  $\alpha K$  clients have the latest sample policy  $\pi'_D$  and  $(1 - \alpha)K$  clients use the old sample policy  $\pi_D$ . Therefore, the virtual global sample policy is given as:

$$\bar{\pi}_D = \frac{1}{K} \left[ \sum_{k=1}^{\alpha K} \pi'_D + \sum_{k=1}^{(1-\alpha)K} \pi_D \right] = \alpha \pi'_D + (1 - \alpha) \pi_D. \quad (8)$$

Using the the definition of  $\Gamma$ :

$$\begin{aligned} \Gamma &:= \sum_{k=1}^K D_{\text{TV}}(\bar{\pi}_D || \pi_D^k) \\ &= \sum_{k=1}^{\alpha K} D_{\text{TV}}(\bar{\pi}_D || \pi'_D) + \sum_{k=1}^{(1-\alpha)K} D_{\text{TV}}(\bar{\pi}_D || \pi_D). \end{aligned} \quad (9)$$

Replacing  $\bar{\pi}$  using Eq. (8), we have for the synchronised component:

$$\begin{aligned} D_{\text{TV}}(\bar{\pi}_D || \pi'_D) &= \frac{1}{2} \sum_{s,a} |\alpha \pi'_D + (1 - \alpha) \pi_D - \pi'_D| \\ &= \frac{1}{2} (1 - \alpha) D_{\text{TV}}(\pi_D || \pi'_D). \end{aligned} \quad (10)$$

Similarly, for the unsynchronised component:

$$\begin{aligned} D_{\text{TV}}(\bar{\pi}_D || \pi_D) &= \frac{1}{2} \sum_{s,a} |\alpha \pi'_D + (1 - \alpha) \pi_D - \pi_D| \\ &= \frac{1}{2} \alpha D_{\text{TV}}(\pi_D || \pi'_D). \end{aligned} \quad (11)$$

Combining Eqs. (9), (10), and (11), we have

$$\Gamma = \alpha(1 - \alpha) K D_{\text{TV}}(\pi_D || \pi'_D). \quad (12)$$

Eq. (12), shows that  $\Gamma$  is influenced both by the policy discrepancy  $D_{\text{TV}}(\pi_D || \pi'_D)$  and the policy synchronous rate  $\alpha$ .  $\Gamma$  takes the maximal value with respect to  $\alpha$  at  $\alpha = 0.5$ . For this value, we would expect the convergence of FEMRL to be most hindered due to highly heterogeneous clients. In the next section, we will show how the degree of non-IID of clients' data distributions affects the rate of the reward improvement for FEMRL.

## V. EXPERIMENTAL EVALUATION

In this section, we aim to evaluate the performance of FEMRL on four realistic continuous control tasks from the rllab framework [13]: HalfCheetah, Ant, Hopper, and Swimmer. For all these tasks, we set the maximal episode length to 500. The details of experiment setup are given in Appendix C.

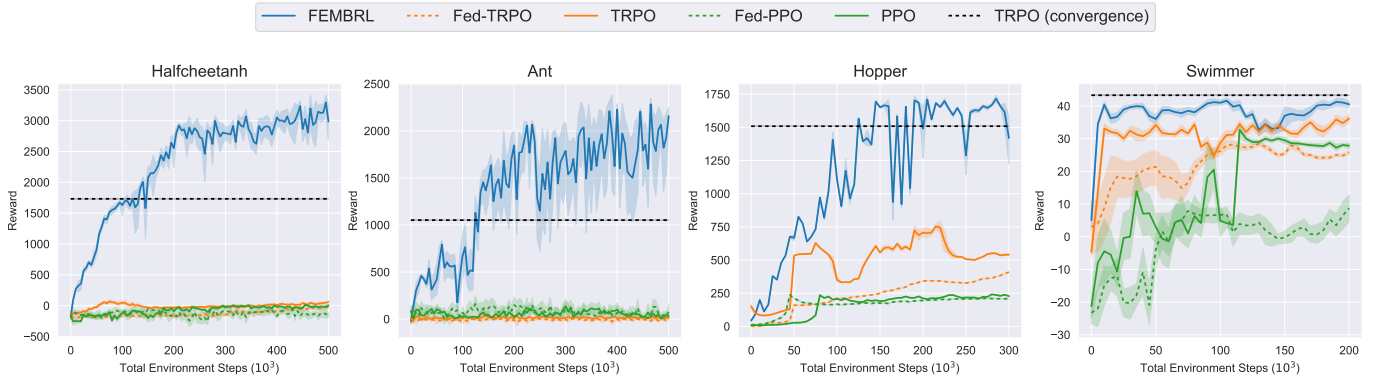


Figure 2: Global total reward during training for FEMRL (blue) and the four baselines on continuous control benchmarks. Solid curves show the average over 10 trials, and shaded regions show the standard deviation of the mean. The dotted horizontal lines give the final total reward of TRPO after 5 million environment steps.

### A. Comparative assessment

We first compare the sampling efficiency of FEMRL to 4 other algorithms: 1) TRPO [33], a model-free policy-gradient based algorithm running centrally, where all client samples are collected on the server (thus breaking the FL assumption). The policy is updated using the gathered samples. 2) Proximal Policy Optimisation (PPO) [36], a model-free RL algorithm also running centrally. 3) Federated TRPO (Fed-TRPO), where each client collects samples from the environment and updates the local policy based on the collected samples. After the local update of the policies on the clients, the server averages all uploaded client policies, creating a global policy for the next round of training. 4) Federated PPO (Fed-PPO), again applying PPO to the FL setting. Both Fed-TRPO and Fed-PPO are federated model-free RL methods. The existing federated RL methods, e.g., [6], [14], [8], share the same FL architecture as Fed-TRPO and Fed-PPO, but differ in the model-free RL algorithm used.

In FEMRL, after the policy update on the server, the parameters of the policy network are sent to clients to update their local policies. However, the update of local policies at clients can be asynchronous: some clients receive the updated policy, others do not receive it and thus will use the old policy for sampling. As a consequence, clients will have heterogeneous sampling policies. We denote the policy synchronous rate as  $\alpha$ , where only  $\alpha K$  clients will receive the updated sample policy at each training epoch. As the default setting of FEMRL, we set  $\alpha = 0.3$ , the number of local update steps of FL  $E = 80$ , and the number of FL communication rounds  $T_c = 5$ . We use  $K = 10$  clients for all algorithms. Each client performs 500 environment steps at each epoch, which therefore has 5000 total environment steps. FEMRL first trains the dynamics model based on the sampled data, and then uses this model to generate fictitious data for policy updating. In contrast, the model-free algorithms (i.e., TRPO, PPO, Fed-TRPO, Fed-PPO) directly use the sampled data for policy update. Due to the sparse reward signal of RL, they generally require huge numbers of interactions with the environment to obtain effective policies, leading to sample inefficiency.

Fig. 2 shows the policy improvement rate of FEMRL and

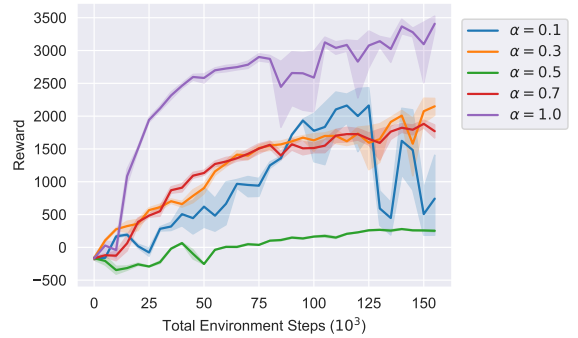


Figure 3: Performance of FEMRL with different policy synchronous rates (i.e.,  $\alpha$ ) on HalfCheetah.

the four baseline algorithms. The dotted lines demonstrate the final performance of (centralised) TRPO after 5 million environment steps. The performance of (centralised) TRPO or PPO acts as a soft upper bound of the federated counterpart (i.e., Fed-TRPO, or Fed-PPO). FEMRL learns substantially faster and achieves the best performance with 0.5 million or fewer environment steps. For example, FEMRL achieves the same performance at 120k environment steps as TRPO does after 5 million environment steps in the HalfCheetah and Ant environments.

### B. The impact of non-IID client data

Clients with non-IID datasets possess unique, non-identical minimisers to their local objectives. During the local-update phase of FL, each participating client’s model will diverge from the global model and move towards their local minimiser. This divergence is termed ‘client-drift’ [37] and has been extensively shown to harm the performance of the global model. The greater the degree of non-IID client data, and the more local steps clients perform, the greater the level of client-drift. In this section, we investigate how non-IID client data impacts the performance of FEMRL.

Eq. (12) shows that the degree of non-IID is determined by  $\alpha$  for FEMRL. Therefore, we evaluate FEMRL with varying



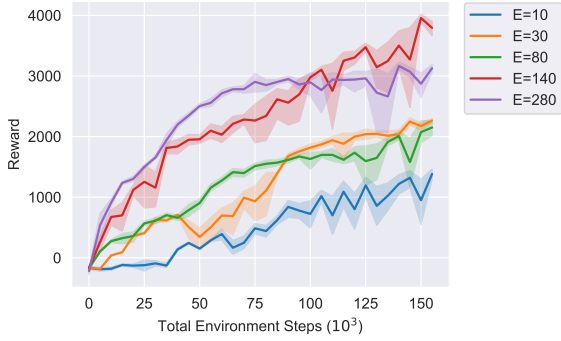


Figure 4: Performance of FEMRL with different numbers of local update steps (i.e.,  $E$ ) on HalfCheetah.

$\alpha$  on HalfCheetah and Fig. 3 shows the training curves. When  $\alpha = 0.5$ , the rate of policy improvement is slowest due to the highly non-IID client data: higher model error results in a worse policy. The rate of policy improvement naturally is the fastest when  $\alpha = 1.0$ , as  $\Gamma$  is 0 (according to Eq. (12)) that represents an IID scenario. When  $\alpha = 0.1$ , although  $\Gamma$  is small, performance is still low because the discrepancy (i.e.,  $\epsilon_\pi$ ) between the sample policy and target policy is large. Lemma IV.1 reveals the relationship between  $\epsilon_\pi$  and the returns of the dynamics model and the real environment. The  $\alpha \in \{0.3, 0.7\}$  curves show that the policy improvement rate of FEMRL falls gracefully as  $\alpha \rightarrow 0.5$ .

### C. The impact of local update steps

Previous works have shown that the number of local steps of SGD that clients perform,  $E$ , is a key factor affecting the convergence of FL algorithms [1], [27], [37]. Larger  $E$  allows clients to do more work locally and make more progress, but the final performance of the global model is harmed when the data on clients is non-IID.

Fig. 4 shows the convergence of FEMRL with a varying number of local steps  $E$ , for a fixed number of communication rounds  $T_c = 5$ . As expected, as  $E$  increases, the initial rate of policy improvement increases as clients make more progress in training the dynamics model. However, as  $E$  becomes very large ( $E = 280$ ), the final reward plateaus at 3000, as the environment model reaches a local optimum and the minimum error it can achieve is harmed. In this scenario, the value of  $E = 140$  strikes a good trade-off between policy improvement rate and maximum reward.

## VI. CONCLUSION

In this paper, we proposed a novel federated RL algorithm: Federated Ensemble Model-based Reinforcement Learning (FEMRL), which incorporates model-based reinforcement learning, and ensemble distillation technologies into FL. In FEMRL, clients train their local dynamics model based on their locally sampled data. An ensemble of the dynamics models is then created at the server based on the updated local models. We use the ensemble model for both policy training and FL model aggregation (by an ensemble distillation method). The updated

policy is then sent to clients for the next-round of sampling process. We provide a rigorous theoretical analysis to prove the monotonic improvement of FEMRL in federated setting with non-IID client data. Finally, we evaluate FEMRL based on four challenging continuous control tasks. Experiment results demonstrate that FEMRL can achieve much higher sample efficiency than federated model-free counterparts.

## REFERENCES

- [1] B. McMahan, E. Moore, D. Ramage, and B. A. y Arcas, "Communication-efficient learning of deep networks from decentralized data," *Proc. International Conference on Artificial Intelligence and Statistics (AISTATS)*, 2017.
- [2] S. J. Reddi, Z. Charles, M. Zaheer, Z. Garrett, K. Rush, J. Konečný, S. Kumar, and H. B. McMahan, "Adaptive federated optimization," in *Proc. International Conference on Learning Representations (ICLR)*, 2021.
- [3] X. Li, K. Huang, W. Yang, S. Wang, and Z. Zhang, "On the convergence of fedavg on non-iid data," in *Proc. International Conference on Learning Representations (ICLR)*, 2020.
- [4] P. Kairouz, H. B. McMahan *et al.*, "Advances and open problems in federated learning," *Foundations and Trends in Machine Learning*, vol. 14, no. 1-2, pp. 1–210, 2021.
- [5] X. Wang, C. Wang, X. Li, V. Leung, and T. Taleb, "Federated deep reinforcement learning for internet of things with decentralized cooperative edge caching," *IEEE Internet of Things Journal*, vol. 7, no. 10, pp. 9441–9455, 2020.
- [6] H. H. Zhuo, W. Feng, Q. Xu, Q. Yang, and Y. Lin, "Federated reinforcement learning," *arXiv preprint arXiv:1901.08277*, 2019.
- [7] C. Nadiger, A. Kumar, and S. Abdelhak, "Federated reinforcement learning for fast personalization," in *IEEE International Conference on Artificial Intelligence and Knowledge Engineering (AIKE)*, 2019, pp. 123–127.
- [8] B. Liu, L. Wang, and M. Liu, "Lifelong federated reinforcement learning: a learning architecture for navigation in cloud robotic systems," *IEEE Robotics and Automation Letters*, vol. 4, no. 4, pp. 4555–4562, 2019.
- [9] X. Liang, Y. Liu, T. Chen, M. Liu, and Q. Yang, "Federated transfer reinforcement learning for autonomous driving," *arXiv preprint arXiv:1910.06001*, 2019.
- [10] M. Janner, J. Fu, M. Zhang, and S. Levine, "When to trust your model: Model-based policy optimization," in *Proc. Advances in Neural Information Processing Systems (NeurIPS)*, vol. 32, 2019.
- [11] T. Kurutach, I. Clavera, Y. Duan, A. Tamar, and P. Abbeel, "Model-ensemble trust-region policy optimization," in *Proc. International Conference on Learning Representations (ICLR)*, 2018.
- [12] L. Kaiser, M. Babaeizadeh, P. Milos *et al.*, "Model based reinforcement learning for atari," in *Proc. International Conference on Learning Representations (ICLR)*, 2020.
- [13] Y. Duan, X. Chen, R. Houthoofd, J. Schulman, and P. Abbeel, "Benchmarking deep reinforcement learning for continuous control," in *Proc. International Conference on Machine Learning (ICML)*, vol. 48, 2016, pp. 1329–1338.
- [14] X. Wang, R. Li, C. Wang, X. Li, T. Taleb, and V. C. M. Leung, "Attention-weighted federated deep reinforcement learning for device-to-device assisted heterogeneous collaborative edge caching," *IEEE Journal on Selected Areas in Communications*, vol. 39, no. 1, pp. 154–169, Jan 2021.
- [15] Y. Zhang, I. Clavera, B. Tsai, and P. Abbeel, "Asynchronous methods for model-based reinforcement learning," in *Proc. Conference on Robot Learning (CoRL)*, vol. 100, 2020, pp. 1338–1347.
- [16] M. Deisenroth and C. E. Rasmussen, "Pilco: A model-based and data-efficient approach to policy search," in *Proc. International Conference on Machine Learning (ICML)*, 2011, pp. 465–472.
- [17] S. Levine and P. Abbeel, "Learning neural network policies with guided policy search under unknown dynamics," in *Proc. Advances in Neural Information Processing Systems (NeurIPS)*, vol. 27, 2014.
- [18] Y. Tassa, T. Erez, and E. Todorov, "Synthesis and stabilization of complex behaviors through online trajectory optimization," in *Proc. IEEE International Conference on Intelligent Robots and Systems (IROS)*, 2012, pp. 4906–4913.
- [19] S. Khansari-Zadeh and A. Billard, "Learning stable nonlinear dynamical systems with gaussian mixture models," *IEEE Transactions on Robotics*, vol. 27, no. 5, pp. 943–957, 2011.

- [20] S. Depeweg, J. M. Hernández-Lobato, F. Doshi-Velez, and S. Udluft, “Learning and policy search in stochastic dynamical systems with bayesian neural networks,” in *Proc. International Conference on Learning Representations (ICLR)*, 2017.
- [21] A. Draeger, S. Engell, and H. Ranke, “Model predictive control using neural networks,” *IEEE Control Systems Magazine*, vol. 15, no. 5, pp. 61–66, 1995.
- [22] A. Nagabandi, G. Kahn, R. Fearing, and S. Levine, “Neural network dynamics for model-based deep reinforcement learning with model-free fine-tuning,” in *Proc. IEEE International Conference on Robotics and Automation (ICRA)*, 2018, pp. 7559–7566.
- [23] K. Chua, R. Calandra, R. McAllister, and S. Levine, “Deep reinforcement learning in a handful of trials using probabilistic dynamics models,” in *Proc. Advances in Neural Information Processing Systems (NeurIPS)*, vol. 31, 2018.
- [24] Y. Luo, H. Xu, Y. Li, Y. Tian, T. Darrell, and T. Ma, “Algorithmic framework for model-based deep reinforcement learning with theoretical guarantees,” in *Proc. International Conference on Learning Representations (ICLR)*, 2019.
- [25] W. Sun, G. J. Gordon, B. Boots, and J. A. Bagnell, “Dual policy iteration,” in *Proc. Advances in Neural Information Processing Systems (NeurIPS)*, vol. 31, 2018.
- [26] R. Kidambi, A. Rajeswaran, P. Netrapalli, and T. Joachims, “Morel: Model-based offline reinforcement learning,” in *Proc. Advances in Neural Information Processing Systems (NeurIPS)*, vol. 33, 2020.
- [27] K. Hsieh, A. Phanishayee, O. Mutlu, and P. Gibbons, “The non-IID data quagmire of decentralized machine learning,” in *Proc. International Conference on Machine Learning (ICML)*, vol. 119, Jul 2020, pp. 4387–4398.
- [28] H.-Y. Chen and W.-L. Chao, “Fedbe: Making bayesian model ensemble applicable to federated learning,” in *Proc. International Conference on Learning Representations (ICLR)*, 2021.
- [29] T. Lin, L. Kong, S. Stich, and M. Jaggi, “Ensemble distillation for robust model fusion in federated learning,” in *Proc. Advances in Neural Information Processing Systems (NeurIPS)*, vol. 33, 2020.
- [30] N. I. Mowla, N. H. Tran, I. Doh, and K. Chae, “Afrl: Adaptive federated reinforcement learning for intelligent jamming defense in fanet,” *Journal of Communications and Networks*, vol. 22, no. 3, pp. 244–258, 2020.
- [31] S. Yu, X. Chen, Z. Zhou, X. Gong, and D. Wu, “When deep reinforcement learning meets federated learning: Intelligent multitimescale resource management for multiaccess edge computing in 5g ultradense network,” *IEEE Internet of Things Journal*, vol. 8, no. 4, pp. 2238–2251, 2020.
- [32] D. P. Kingma and J. Ba, “Adam: A method for stochastic optimization,” in *Proc. International Conference on Learning Representations (ICLR)*, 2015.
- [33] J. Schulman, S. Levine, P. Abbeel, M. Jordan, and P. Moritz, “Trust region policy optimization,” in *Proc. International Conference on Machine Learning (ICML)*, vol. 37, 2015, pp. 1889–1897.
- [34] S. Shalev-Shwartz and S. Ben-David, *Understanding machine learning: From theory to algorithms*. Cambridge University Press, 2014.
- [35] T. Yu, G. Thomas, L. Yu, S. Ermon, J. Y. Zou, S. Levine, C. Finn, and T. Ma, “Mopo: Model-based offline policy optimization,” in *Proc. Advances in Neural Information Processing Systems (NeurIPS)*, vol. 33, 2020.
- [36] J. Schulman, F. Wolski, P. Dhariwal, A. Radford, and O. Klimov, “Proximal policy optimization algorithms,” *arXiv preprint arXiv:1707.06347*, 2017.
- [37] S. P. Karimireddy, S. Kale, M. Mohri, S. Reddi, S. Stich, and A. T. Suresh, “SCAFFOLD: Stochastic controlled averaging for federated learning,” in *Proc. International Conference on Machine Learning (ICML)*, vol. 119, 2020, pp. 5132–5143.
- [38] M. Mohri, A. Rostamizadeh, and A. Talwalkar, *Foundations of machine learning*. MIT press, 2018.
- [39] J. Schulman, P. Moritz, S. Levine, M. Jordan, and P. Abbeel, “High-dimensional continuous control using generalized advantage estimation,” *arXiv preprint arXiv:1506.02438*, 2015.



## APPENDIX

## A. Lemmas

In this section, we provide some useful Lemmas for the theoretical analysis of monotonic improvement guarantee for FEMRL.

**Lemma A.1.** (*Importance sampling inequality*) For any distribution  $\rho(s)$  and  $\rho'(s)$  and a function  $f(s)$ , we have  $\mathbb{E}_{s \sim \rho(s)} f(s) \leq \mathbb{E}_{s \sim \rho'(s)} f(s) + |\rho(s) - \rho'(s)| f_{\max}$ , where  $f_{\max}$  is the maximal value of  $f(s)$ .

*Proof.*

$$\begin{aligned} \mathbb{E}_{s \sim \rho(s)} f(s) &= \mathbb{E}_{s \sim \rho'(s)} \frac{\rho(s)}{\rho'(s)} f(s) = \mathbb{E}_{s \sim \rho'(s)} \frac{\rho(s) - \rho'(s) + \rho'(s)}{\rho'(s)} f(s) \\ &= \mathbb{E}_{s \sim \rho'(s)} f(s) + \mathbb{E}_{s \sim \rho'(s)} (\rho(s) - \rho'(s)) f(s) \\ &\leq \mathbb{E}_{s \sim \rho'(s)} f(s) + \sum_s |\rho(s) - \rho'(s)| f_{\max} \\ &\leq \mathbb{E}_{s \sim \rho'(s)} f(s) + \|\rho(s) - \rho'(s)\|_1 f_{\max}. \end{aligned}$$

□

**Lemma A.2.** (*Bounded difference of discounted state distributions*). Let  $\pi$  and  $\pi_D$  be two different policies and  $\epsilon_\pi = D_{\text{TV}}(\pi || \pi_D)$ , we have:

$$\|\rho_\pi^{\mathcal{M}} - \rho_{\pi_D}^{\mathcal{M}}\|_1 \leq \frac{2\gamma}{(1-\gamma)^2} \epsilon_\pi.$$

*Proof.* Define  $\mathbb{P}_\pi^{\mathcal{M}}$  and  $\mathbb{P}_{\pi_D}^{\mathcal{M}}$  as the transition kernels of the MDP  $\mathcal{M}$  following policies  $\pi$  and  $\pi_D$ , respectively. Let  $\mathbf{G} = (\mathbf{I} + \gamma \mathbb{P}_\pi^{\mathcal{M}} + (\gamma \mathbb{P}_\pi^{\mathcal{M}})^2 + \dots) = (\mathbf{I} - \gamma \mathbb{P}_\pi^{\mathcal{M}})^{-1}$  and  $\mathbf{G}_D = (\mathbf{I} + \gamma \mathbb{P}_{\pi_D}^{\mathcal{M}} + (\gamma \mathbb{P}_{\pi_D}^{\mathcal{M}})^2 + \dots) = (\mathbf{I} - \gamma \mathbb{P}_{\pi_D}^{\mathcal{M}})^{-1}$ . Let  $\mathbf{\Delta} = \mathbb{P}_{\pi_D}^{\mathcal{M}} - \mathbb{P}_\pi^{\mathcal{M}}$ . We start with some algebraic manipulations as:

$$\mathbf{G}^{-1} - \mathbf{G}_D^{-1} = (\mathbf{I} - \gamma \mathbb{P}_\pi^{\mathcal{M}}) - (\mathbf{I} - \gamma \mathbb{P}_{\pi_D}^{\mathcal{M}}) = \gamma \mathbf{\Delta}.$$

Left-multiplying by  $\mathbf{G}$  and right-multiplying by  $\mathbf{G}_D$ , then multiplying by  $\rho_0$ :

$$\mathbf{G}_D \rho_0 - \mathbf{G} \rho_0 = \gamma \mathbf{G} \mathbf{\Delta} \mathbf{G}_D \rho_0.$$

Note that  $\rho_\pi^{\mathcal{M}} = \mathbf{G} \rho_0$ . By definition we have  $\|\mathbf{G}\|_1 = (1-\gamma)^{-1}$ ,  $\|\mathbf{\Delta}\|_1 = 2D_{\text{TV}}(\pi || \pi_D)$ , and  $\|\rho_0\| = 1$ . Hence:

$$\begin{aligned} \|\rho_\pi^{\mathcal{M}} - \rho_{\pi_D}^{\mathcal{M}}\|_1 &= \|\gamma \mathbf{G} \mathbf{\Delta} \mathbf{G}_D \rho_0\|_1 \leq \gamma \|\mathbf{G}\|_1 \|\mathbf{\Delta}\|_1 \|\mathbf{G}_D\|_1 \|\rho_0\|_1 \\ &\leq \frac{2\gamma}{(1-\gamma)^2} D_{\text{TV}}(\pi || \pi_D) = \frac{2\gamma}{(1-\gamma)^2} \epsilon_\pi. \end{aligned}$$

□

## B. Proof of Lemma IV.1

*Proof.* Let  $\rho_\pi^{\mathcal{M}}$  be the discounted visitation frequencies [33] over the state space as  $\rho_\pi^{\mathcal{M}}(s) = \sum_{t=0}^{\infty} \gamma^t P(S_t = s | \pi, \mathcal{M})$ , where  $P(S_t = s | \pi, \mathcal{M})$  denotes the probability of being in state  $s$  at time step  $t$  in the MDP  $\mathcal{M} := (\mathcal{S}, \mathcal{A}, T, R, \rho_0, \gamma)$  following the policy  $\pi$ . We can define the expected discounted return as:

$$\begin{aligned} V_\pi^{\mathcal{M}} &= \mathbb{E}_{\substack{S_{t+1} \sim T(\cdot | S_t, A_t) \\ A_t \sim \pi(\cdot | S_t)}} \left[ \sum_{t=0}^{\infty} \gamma^t R(S_t, A_t) \middle| S_0 = s_0 \right] \\ &= \mathbb{E}_{s \sim \rho_\pi^{\mathcal{M}}(s), a \sim \pi(a|s)} [R(s, a)], \end{aligned} \tag{13}$$

where  $s_0$  is the initial state.

Let  $W_j$  be the discounted total reward when executing  $\pi$  on the dynamics model  $\mathcal{M}$  for the first  $j$  steps and the rest of the steps on  $\widehat{\mathcal{M}}$ . That is:

$$W_j = \mathbb{E}_{\substack{\forall t \geq 0, A_t \sim \pi(\cdot | S_t) \\ \forall j > t \geq 0, S_{t+1} \sim T(\cdot | S_t, A_t) \\ \forall t \geq j, S_{t+1} \sim \widehat{T}(\cdot | S_t, A_t)}} \left[ \sum_{t=0}^{\infty} \gamma^t R(S_t, A_t) \middle| S_0 = s_0 \right].$$

Note that we define  $V_\pi^{\mathcal{M}} = \mathbb{E}_{s_0 \sim \rho_0} [V_\pi^{\mathcal{M}}(s_0)]$ . By definition we have  $W_\infty = V_\pi^{\mathcal{M}}$  and  $W_0 = V_\pi^{\widehat{\mathcal{M}}}$ , thus:

$$V_\pi^{\widehat{\mathcal{M}}} - V_\pi^{\mathcal{M}} = \sum_{j=0}^{\infty} (W_{j+1} - W_j).$$

We rewrite  $W_j$  and  $W_{j+1}$  as:

$$W_j = R_j + \mathbb{E}_{A_j, S_j \sim \pi, T} \left[ \mathbb{E}_{\hat{S}_{j+1} \sim \hat{T}(\cdot | S_j, A_j)} \left[ \gamma^{j+1} V_{\pi}^{\widehat{\mathcal{M}}}(\hat{S}_{j+1}) \right] \right],$$

$$W_{j+1} = R_j + \mathbb{E}_{A_j, S_j \sim \pi, T} \left[ \mathbb{E}_{S_{j+1} \sim T(\cdot | S_j, A_j)} \left[ \gamma^{j+1} V_{\pi}^{\mathcal{M}}(S_{j+1}) \right] \right].$$

Therefore:

$$W_{j+1} - W_j = \gamma^{j+1} \mathbb{E}_{A_j, S_j \sim \pi, T} \left[ \mathbb{E}_{S_{j+1} \sim T(\cdot | S_j, A_j)} \left[ V_{\pi}^{\mathcal{M}}(S_{j+1}) \right] - \mathbb{E}_{\hat{S}_{j+1} \sim \hat{T}(\cdot | S_j, A_j)} \left[ V_{\pi}^{\widehat{\mathcal{M}}}(\hat{S}_{j+1}) \right] \right]$$

$$= \gamma^{j+1} \mathbb{E}_{A_j, S_j \sim \pi, T} \left[ G_{\widehat{\mathcal{M}}}^{\pi}(S, A) \right],$$

where  $R_j$  is the expected accumulative reward of the first  $j$  steps, which are taken w.r.t. dynamics model  $\mathcal{M}$ . Thus we have:

$$V_{\pi}^{\widehat{\mathcal{M}}} - V_{\pi}^{\mathcal{M}} = \sum_{j=0}^{\infty} (W_{j+1} - W_j)$$

$$= \sum_{j=0}^{\infty} \gamma^{j+1} \mathbb{E}_{A_j, S_j \sim \pi, T} \left[ G_{\widehat{\mathcal{M}}}^{\pi}(S, A) \right]$$

$$= \gamma \mathbb{E}_{\substack{S \sim \rho_{\pi}^{\mathcal{M}}, \\ A \sim \pi(\cdot | S)}} \left[ G_{\widehat{\mathcal{M}}}^{\pi}(S, A) \right],$$

where the last equality is from applying Eq. (13), and we define  $G_{\widehat{\mathcal{M}}}^{\pi}(S, A) = \mathbb{E}_{S' \sim T(\cdot | S, A)} \left[ V_{\pi}^{\mathcal{M}}(S') \right] - \mathbb{E}_{\hat{S}' \sim \hat{T}(\cdot | S, A)} \left[ V_{\pi}^{\widehat{\mathcal{M}}}(\hat{S}') \right]$ .

For simplicity, we define  $T(S, A) = T(s'|s, a)$  as the dynamics of the real environment and  $\hat{T}(S, A) = \hat{T}(s'|s, a)$  as the dynamics of the learned model. The reward function is bounded by  $r_{\max}$  according to Assumption 3, we then have for any value function:  $\|V_{\pi}\| \leq \frac{1}{1-\gamma} r_{\max}$ . Next, we bound  $G_{\widehat{\mathcal{M}}}^{\pi}(S, A)$  as:

$$G_{\widehat{\mathcal{M}}}^{\pi}(S, A) = \sum_{S'} T(S, A) V_{\pi}^{\mathcal{M}}(S') - \sum_{S'} \hat{T}(S, A) V_{\pi}^{\widehat{\mathcal{M}}}(S')$$

$$\leq \frac{r_{\max}}{1-\gamma} \sum_{S'} \left[ T(S, A) - \hat{T}(S, A) \right]$$

$$\leq \frac{2r_{\max}}{1-\gamma} D_{\text{TV}}(T(S, A) \| \hat{T}(S, A)).$$

Therefore:

$$V_{\pi}^{\widehat{\mathcal{M}}} - V_{\pi}^{\mathcal{M}} \leq \frac{2\gamma r_{\max}}{1-\gamma} \mathbb{E}_{\substack{S \sim \rho_{\pi}^{\mathcal{M}}, \\ A \sim \pi(\cdot | S)}} \left[ D_{\text{TV}}(T(S, A) \| \hat{T}(S, A)) \right]. \quad (14)$$

We define  $\epsilon_m = \mathbb{E}_{S \sim \rho_{\pi_D}^{\mathcal{M}}, A \sim \pi(\cdot | S)} \left[ D_{\text{TV}}(T(S, A) \| \hat{T}(S, A)) \right]$  and  $\epsilon_m^{\max} = \max_{S \sim \rho_{\pi_D}^{\mathcal{M}}} \left[ D_{\text{TV}}(T(S, A) \| \hat{T}(S, A)) \right]$ . In our algorithm we use the sample policy  $\pi_D$  to sample trajectories from the real environment, so we bound the following using **Lemma A.1** and **Lemma A.2** as:

$$\mathbb{E}_{\substack{S \sim \rho_{\pi}^{\mathcal{M}}, \\ A \sim \pi(\cdot | S)}} \left[ D_{\text{TV}}(T(S, A) \| \hat{T}(S, A)) \right] \leq \mathbb{E}_{\substack{S \sim \rho_{\pi_D}^{\mathcal{M}}, \\ A \sim \pi(\cdot | S)}} \left[ D_{\text{TV}}(T(S, A) \| \hat{T}(S, A)) \right]$$

$$+ \|\rho_{\pi}^{\mathcal{M}} - \rho_{\pi_D}^{\mathcal{M}}\|_1 \max_{S \sim \rho_{\pi_D}^{\mathcal{M}}} \left[ D_{\text{TV}}(T(S, A) \| \hat{T}(S, A)) \right]$$

$$\leq \epsilon_m + \frac{2\gamma}{(1-\gamma)^2} \epsilon_{\pi} \epsilon_m^{\max}.$$

Combining the above inequality with Eq. (14), we have:

$$V_{\pi}^{\widehat{\mathcal{M}}} - V_{\pi}^{\mathcal{M}} \leq \frac{2\gamma r_{\max}}{1-\gamma} \epsilon_m + \frac{4\gamma^2 r_{\max}}{(1-\gamma)^3} \epsilon_{\pi} \epsilon_m^{\max}.$$

□

In this section, we derive a bound on the generalisation error of the environment model trained during our FEMRL learning process. Since the training of the model is a supervised learning process, we can utilise the Probably Approximately Correct (PAC) learning framework for our analysis. First, we give the general bounds for Vapnik–Chervonenkis (VC)-dimension learning and the discrepancy of the generalisation error between two different data domains. We then give the proof of Theorem IV.2.

### C. Preliminaries

**Theorem A.3.** (Uniform VC-dimension error bound [38]) Let  $\mathcal{H}$  be a hypothesis class with  $VCdim(\mathcal{H}) \leq d < \infty$ . Let  $D$  be the probability measures over the sample space. Let  $S$  be the empirical dataset sampled from  $D$ ,  $S \sim D^m$  where  $m$  is the size of the dataset. Then for any  $\delta > 0$ , with probability at least  $1 - \delta$ , the following holds for all  $h \in \mathcal{H}$ :

$$|\epsilon_D(h) - \epsilon_S(h)| \leq C \sqrt{\frac{d + \log(1/\delta)}{m}}, \quad (15)$$

where  $C$  is a constant factor.

We now give a bound of learning between different domains.

**Lemma A.4.** Let  $\mathcal{H}$  be a hypothesis class.  $D$  and  $D'$  denote two probability measures over the sample space. Let  $\epsilon_D h$  denote the general error of  $h$  over  $D$ . If the loss function  $l(\cdot)$  is bounded by  $L$ , then for every  $h \in \mathcal{H}$  we have:

$$\epsilon_D(h) \leq \epsilon_{D'}(h) + L\|D - D'\|_1. \quad (16)$$

*Proof.*

$$\begin{aligned} \epsilon_D(h) &\leq \epsilon_{D'}(h) + |\epsilon_D(h) - \epsilon_{D'}(h)| \\ &\leq \epsilon_{D'}(h) + \int |l(y, h(x))| |\mathbb{P}_{(x,y) \sim D} - \mathbb{P}_{(x,y) \sim D'}| \\ &= \epsilon_{D'}(h) + L\|D - D'\|_1. \end{aligned} \quad (17)$$

□

### D. Proof of Theorem IV.2

*Proof.* According to the definition of Empirical Risk Minimisation (ERM), we have  $\epsilon_{S_k}(h_{S_k}) \leq \epsilon_{S_k}(h_{\hat{S}})$ , where  $h_{\hat{S}}$  is the model learned based on the virtual global empirical dataset  $\hat{S}$ , where  $\hat{S} = \frac{1}{K} \sum_{k=1}^K S_k$ . Therefore, we have:

$$\frac{1}{K} \sum_{k=1}^K \epsilon_{S_k}(h_{S_k}) \leq \frac{1}{K} \sum_{k=1}^K \epsilon_{S_k}(h_{\hat{S}}) = \epsilon_{\hat{S}}(h_{\hat{S}}). \quad (18)$$

Next we give the bound of the generalisation error of the model ensemble, by considering the distance between the generalisation error of the ensemble of client models,  $\epsilon_D(\frac{1}{K} \sum_k h_{S_k})$ , and the generalisation error of the model learned from the virtual global dataset,  $\epsilon_D(h_{\hat{S}})$ . By convexity of the loss function  $f$  and Jensen's inequality, we have the probability of at least  $1 - \delta$  over  $\{S_k \sim D_k^m\}_{k=1}^K$  that:

$$\begin{aligned} \epsilon_D \left( \frac{1}{K} \sum_k h_{S_k} \right) &\leq \frac{1}{K} \sum_k \epsilon_D(h_{S_k}) \\ &\leq \frac{1}{K} \sum_k \left( \epsilon_{S_k}(h_{S_k}) + C \sqrt{\frac{d + \log(1/\delta)}{m}} + L\|D - D_k\|_1 \right) \\ &\leq \frac{1}{K} \sum_k \epsilon_{S_k}(h_{S_k}) + C \sqrt{\frac{d + \log(1/\delta)}{m}} + \frac{1}{K} \sum_k L\|D - D_k\|_1 \\ &\leq \epsilon_{\hat{S}}(h_{\hat{S}}) + C \sqrt{\frac{d + \log(1/\delta)}{m}} + \frac{L}{K} \sum_k \|D - D_k\|_1. \end{aligned}$$

The distribution of the virtual global dataset can be calculated using  $D = \mathbb{P}_{s,a,s'} = \sum_{s,a} T(s'|s, a) \bar{\pi}_D(a|s)$ :

$$\begin{aligned} \|D - D_k\|_1 &= \sum_{s',s,a} |\mathbb{P}_{s,a,s' \sim D} - \mathbb{P}_{s,a,s' \sim D_k}| \\ &= \sum_{s'} \sum_{s,a} (T(s'|s, a) \bar{\pi}_D(a|s) - T(s'|s, a) \pi_D^k(a|s)) \\ &= \sum_{s'} T(s'|s, a) \sum_{s,a} (\bar{\pi}_D(a|s) - \pi_D^k(a|s)) \\ &= \sum_{s,a} (\bar{\pi}_D(a|s) - \pi_D^k(a|s)) \\ &= D_{\text{TV}}(\bar{\pi}_D \| \pi_D^k). \end{aligned} \quad (19)$$

Denote the discrepancy between the sample policy of client  $k$ ,  $\pi_D^k$ , and the virtual global sample policy  $\bar{\pi}_D$  as  $D_{\text{TV}}(\bar{\pi}_D || \pi_D^k)$ . Let  $\Gamma = \sum_k D_{\text{TV}}(\bar{\pi}_D || \pi_D^k)$ . Therefore, we have:

$$\epsilon_D \left( \frac{1}{K} \sum_k h_{S_k} \right) \leq \epsilon_{\hat{S}_k}(h_{\hat{S}_k}) + C \sqrt{\frac{d + \log(1/\delta)}{m}} + \frac{L}{K} \Gamma, \quad (20)$$

where  $\Gamma$  can be used to measure the degree of the non-IID client data. □

In this section, we give more details about the experiments presented in the main body of the paper and in the appendix. First, we present the procedure running on the clients during FEMRL (LocalUpdate). Next we give the implementation details about the environment, FEMRL, and baseline algorithms. Finally, we show additional experimental results.

### E. FEMRL: Client side algorithm

Algorithm 2 presents the procedure of FEMRL on client-side. The client first samples trajectories from the real environment using the sample policy, and then collects all the sampled trajectories into the local replay buffer,  $D_k$ . Next, the client conducts  $E$  local update steps to train the local dynamics model with mini-batch gradient descent. The returned local dynamics model is then uploaded to the server for further processing.

---

#### Algorithm 2 Procedures of client side

---

##### Procedure LocalUpdate( $k, \omega_k^0, E$ )

```

Collect trajectories  $(s_t, a_t, s_{t+1})_t$  with  $\pi_\theta$  in the real environment
Store trajectories into the local replay buffer  $D_k \leftarrow D_k \cup (s_t, a_t, s_{t+1})_t$ 
for  $i \leftarrow 1$  to  $E$  do
    Random sample a batch of training data  $\xi_i$  from  $D_k$ 
    Conduct mini-batch gradient descent:  $\omega_k^i \leftarrow \omega_k^{i-1} - \eta_i \nabla f_k(\omega_k^{i-1}; \xi_i)$ 
return  $\omega_k^E$ 

```

---

### F. Implementation details

We evaluate the algorithms on four Mujoco environments: Swimmer, Hopper, Ant, and HalfCheetah. The implementation of the environments are the same as [24], [13]. Specifically, we set the maximal episode length as 500 for all environments.

#### FEMRL:

We implement FEMRL and all baseline algorithms by using Pytorch ( $\geq 1.7.0$ ). Specially, the dynamics of the MDP is approximated by the feed-forward neural network with two hidden layers and each layer includes 500 units. The activation function at each layer is ReLU. Instead of directly predicting the next state, the network predicts the normalised differences between the next state  $s_{t+1}$  and  $s_t$  as in previous works [11], [24]. Each client maintains its own normalised statistics (i.e., the mean  $\mu$ , and standard deviation  $\sigma$ ) based on the sampled local dataset. The normalised difference can be calculated as  $((s_{t+1} - s_t) - \mu) / \sigma$ .

The policy neural network is also implemented by a feed-forward neural network with two hidden layers, each of which has 128 hidden units. We use ReLU as the activation function and the output of the policy neural network is a Gaussian distribution  $\mathcal{N}(\mu(s), \sigma^2)$  where  $\sigma$  is a state-independent trainable vector.

For other default settings of FEMRL, we set the number of inner loops as  $n_{\text{inner}} = 20$  at each training epoch. Each client conducts 500 environment steps using the sample policy and stores the sampled data locally. We set the batch size of local updates for the dynamics model as 128 for all clients. Each client conducts  $E = 80$  steps of local training with Adam (with learning rate  $10^{-3}$ ) and then uploads parameters of the local dynamics model to the server. The server then aggregates the uploaded models into a single global model through knowledge distillation. Specifically, we use the sample policy to sample trajectories based on the ensemble of client models and then apply the student-teacher scheme to train a single global model on the fictional trajectories. The learning rate and batch size of the knowledge distillation are set as  $10^{-3}$  and 128, respectively. At each epoch, we optimise the dynamics model and policy alternatively for  $n_{\text{inner}} = 20$  times. At each inner loop, we conduct  $T_c = 5$  communication rounds between clients and server for training the dynamic models. After the training for the dynamics model, we then use a policy gradient algorithm (TRPO) to train the policy. We set the number of iterations for policy training as  $G = 20$ .

### Baseline algorithms:

For the settings of the model-free baseline algorithms, we use two advanced policy gradient methods: PPO and TRPO. Both PPO and TRPO use General Advantage Estimator (GAE) [39] to measure advantages. The policy networks of all baseline algorithms share the same settings as FEMRL. The hyperparameters settings for centralised TRPO and PPO are listed in Tables I and II, respectively. Fed-TRPO and Fed-PPO share most of the hyperparameters settings as their centralised counterparts except batch size (TRPO) and environment steps per epoch (PPO). Since Fed-TRPO and Fed-PPO do not collect data from clients, thus the batch size of Fed-TRPO on each client is set as 500 while the environment steps per epoch of Fed-PPO on each client is set as 500.

Table I: Hyperparameters for TRPO.

Hyperparameters	Values	Hyperparameters	Values
Batch Size	5000	Max KL Divergence	0.01
Discount $\gamma$	0.99	GAE $\lambda$	0.95
Conjugate Gradient Damping	0.1	Conjugate Gradient Steps	10

Table II: Hyperparameters for PPO.

Hyperparameters	Values	Hyperparameters	Values
Batch Size	100	Environment Steps per Epoch	5000
Learning Rate	0.001	Optimizer	Adam
GAE $\lambda$	0.95	Discount $\gamma$	0.99
Entropy Coefficient	0.01	Clipping Value $\epsilon$	0.2

### G. Extended Experiments

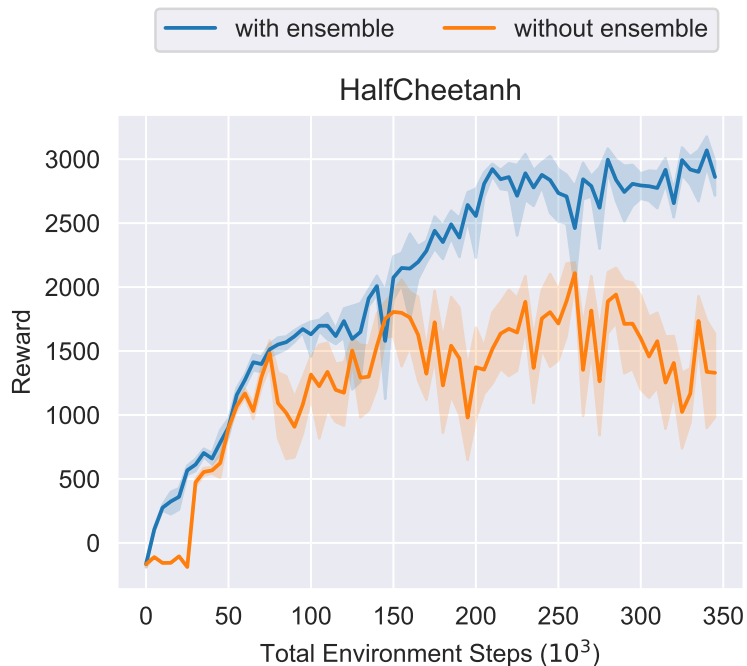


Figure 5: Performance of FEMRL with or without ensemble knowledge distillation on HalfCheetah.

In this section, we conduct extra experiments for an ablation study of FEMRL. We first investigate how the ensemble knowledge distillation method affects the performance. We train FEMRL on HalfCheetah without using ensemble knowledge distillation. Specifically, we directly average the uploaded parameters of clients' models and create a single global dynamics model for the FL training process. After  $T = 5$  rounds of FL training, we use the global dynamics model for the policy-updating process using TRPO. The rest of the hyperparameter settings are the same as the default settings in Section V. Fig 5 shows

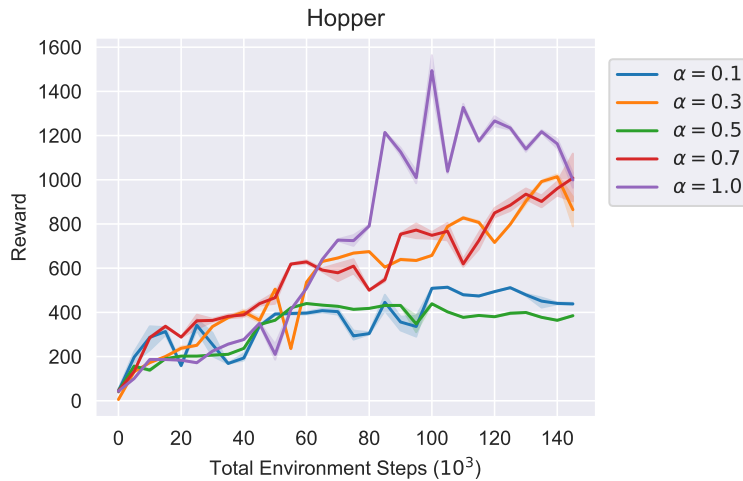


Figure 6: Performance of FEMRL with different policy synchronisation rates (i.e.,  $\alpha$ ) on Hopper.

the results of FEMRL on HalfCheetah with or without ensemble knowledge distillation. We find that the ensemble model distillation method can significantly improve the performance of FEMRL, indicating the importance and necessity of combining ensemble knowledge distillation into our method.

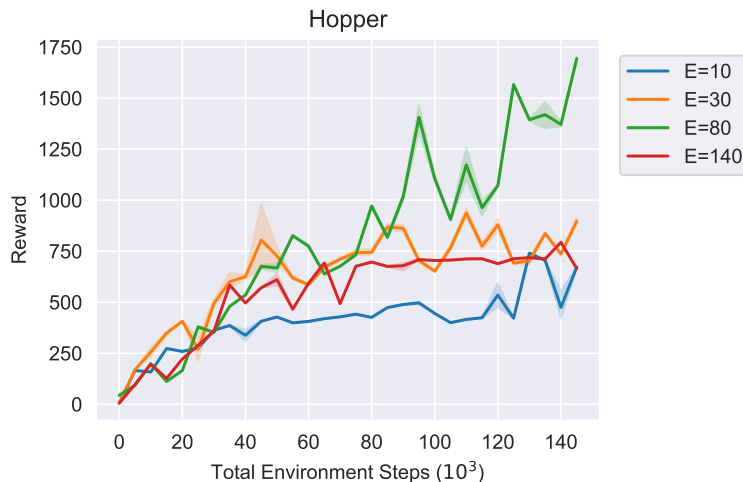


Figure 7: Performance of FEMRL with different numbers of local steps (i.e.,  $E$ ) on Hopper.

Next, we investigate the impact of the policy synchronous rate  $\alpha$  on Hopper. Fig. 6 shows the performance of FEMRL on Hopper with varying policy synchronisation rates. As expected, when  $\alpha = 1.0$ , the client data is purely IID, therefore FEMRL can achieve the best performance. In contrast, when  $\alpha = 0.5$ , the degree of non-IID is maximal, therefore, FEMRL obtains the worst performance.

Fig. 7 shows the performance of FERML on varying numbers of local update steps, for a fixed number of communication rounds  $T_c = 5$ . As expected, both small ( $E = 10, 30$ ) and large ( $E = 140$ ) number of local update steps can harm the convergence rate. The value of  $E = 80$  achieves the best performance in this scenario.